

Magnetic field control of the neutral and charged exciton fine structure in single quantum dashes emitting at 1.55 μm

P. Mrowiński, A. Musiał, A. Maryński, M. Syperek, J. Misiewicz, A. Somers, J. P. Reithmaier, S. Höfling, and G. Sek

Citation: *Applied Physics Letters* **106**, 053114 (2015); doi: 10.1063/1.4907650

View online: <http://dx.doi.org/10.1063/1.4907650>

View Table of Contents: <http://scitation.aip.org/content/aip/journal/apl/106/5?ver=pdfcov>

Published by the [AIP Publishing](#)

Articles you may be interested in

Single photon emission at 1.55 μm from charged and neutral exciton confined in a single quantum dash
Appl. Phys. Lett. **105**, 021909 (2014); 10.1063/1.4890603

Exciton and biexciton dynamics in single self-assembled InAs/InGaAlAs/InP quantum dash emitting near 1.55 μm
Appl. Phys. Lett. **103**, 253113 (2013); 10.1063/1.4852736

Carrier relaxation dynamics in InAs/GaInAsP/InP(001) quantum dashes emitting near 1.55 μm
Appl. Phys. Lett. **103**, 083104 (2013); 10.1063/1.4818759

Fine structural splitting and exciton spin relaxation in single InAs quantum dots
J. Appl. Phys. **105**, 103516 (2009); 10.1063/1.3131700

Manipulating exciton fine structure in quantum dots with a lateral electric field
Appl. Phys. Lett. **90**, 041101 (2007); 10.1063/1.2431758

The advertisement features a photograph of the Model PS-100 cryogenic probe station, which is a complex piece of scientific equipment with various mechanical components and a probe. The background is a gradient of blue. The text is arranged around the image: the model name and description on the left, the company logo and name on the right, and a slogan at the bottom right.

Model PS-100
Tabletop Cryogenic
Probe Station



Lake Shore
CRYOTRONICS

*An affordable solution for
a wide range of research*

Magnetic field control of the neutral and charged exciton fine structure in single quantum dashes emitting at 1.55 μm

P. Mrowiński,¹ A. Musiał,^{1,a)} A. Maryński,¹ M. Syperek,¹ J. Misiewicz,¹ A. Somers,² J. P. Reithmaier,^{2,3} S. Höfling,^{2,4} and G. Sęk¹

¹Laboratory for Optical Spectroscopy of Nanostructures, Department of Experimental Physics, Wrocław University of Technology, Wybrzeże Wyspiańskiego 27, Wrocław, Poland

²Technische Physik, University of Würzburg & Wilhelm-Conrad-Röntgen-Research Center for Complex Material Systems, Am Hubland, D-97074 Würzburg, Germany

³Institute of Nanostructure Technologies and Analytics (INA), CINSaT, University of Kassel, Heinrich-Plett-Str. 40, 34132 Kassel, Germany

⁴SUPA, School of Physics and Astronomy, University of St. Andrews, North Haugh, KY16 9SS St. Andrews, United Kingdom

(Received 14 December 2014; accepted 26 January 2015; published online 5 February 2015)

We investigated the neutral and charged exciton fine structure in single InAs/InGaAlAs/InP quantum dashes emitting at 1.55 μm using polarization-resolved microphotoluminescence in a magnetic field. Inverted spin configuration of horizontally [1–10] and vertically [110] polarized transitions has been observed. An in-plane magnetic field of up to 5 Tesla has been applied to tailor the fine structure, and eventually to reduce the splitting of the bright exciton states down to zero. This inverted structure has been observed for all the investigated excitons, making it a characteristic feature for this class of nanostructures with the largest splitting reduction of 170 μeV . © 2015 AIP Publishing LLC.
[\[http://dx.doi.org/10.1063/1.4907650\]](http://dx.doi.org/10.1063/1.4907650)

In-plane shape asymmetry and anisotropy of the strain in self-assembled quantum dots, resulting in the confinement potential anisotropy, are the main structural reasons of the so-called fine structure splitting (FSS) of the bright exciton states via the long-range spin-exchange interaction. Engineering the FSS value and understanding the underlying physics have attracted a lot of attention in the past few years as it is a crucial “tuning knob” in quantum communication,¹ quantum computing,² or quantum cryptography systems³ and their realization in a solid state platform. Reduction of the splitting below the natural lifetime-limited spectral width of the single exciton state enables generation of entangled photon pairs from a single quantum dot using biexciton-exciton cascade.^{4,5} This scheme is a promising alternative to parametric down-conversion processes,⁶ due to the possibility of on-demand operation under pulsed excitation and sub-Poissonian statistics of the emitted photons.

As the control of the FSS by tailoring self-assembled growth is challenging,⁷ an enormous effort has been made towards development of post-growth tuning mechanisms in order to increase the fidelity of entanglement of emitted photons. Several strategies for FSS manipulation have been tested including an in-plane or vertical electric field,^{5,8} external magnetic field,⁹ uniaxial stress,^{10,11} or structure annealing.¹² A complete elimination of FSS, however, is not always achievable. For example, strain tuning suffers from fundamental limitations that have been theoretically predicted¹³ and experimentally verified,^{14,15} whereas annealing cannot be applied locally and is very inefficient: it relies on minimizing the FSS over the ensemble and subsequently identifying zero-value cases. An alternative that avoids

these disadvantages is exploiting the crossing between bright exciton states using an external perturbation, such as in-plane magnetic field. In this case, one more additional requirement must be fulfilled, namely, the inverted fine structure making FSS¹⁶ negative, which is thought to be related to atypical expansion of electron and hole wavefunctions as a result of interplay between the confinement and piezoelectric field. Although the concept of reducing the FSS in inverted spin configuration structure by magnetic field was already utilized,¹⁷ FSS crossing was reached for less than 30% of the dots, which indicates that post selection is a limiting factor. Suggestions that the heavy-hole light-hole mixing effect is responsible for a sign change¹⁸ makes strongly elongated nanostructures very promising candidates, while a non-zero degree of linear polarization reflecting strong light-hole admixture^{19,20} has been reported recently.²¹

Therefore, our attention is focused on InAs/InGaAlAs/InP quantum dashes (QDashes) elongated in [1–10] crystallographic direction. They have this advantage that they can be designed to emit in the 1.55 μm spectral range,²² particularly interesting for data transmission at the C-band telecommunication window. It has recently been proven that a single quantum dash can act as an effective single photon emitter, both from neutral exciton and charged exciton complex,²³ which further increases the motivation for this research. Magneto-optical spectroscopy has been very widely used and shown as a comprehensive method for studying the fundamental properties of self-assembled quantum dots.^{24–27} This technique gives insight into the spin degree of freedom of the confined charge carriers which can be initialized by optical means, and then utilized in spintronics and spin-based quantum information processing.^{28–30} Moreover, if the magnetic field is employed as a photon entanglement tool

^{a)}Current address: Institut für Festkörperphysik, Technische Universität Berlin, Hardenbergstraße 36, D-10623 Berlin, Germany.

combined with a mature semiconductor technology, it could start a modern concept of the on-chip FSS tuning: for instance, using the manganese-induced micromagnetism that is able to generate locally about 0.5 T.

The sample investigated contains a layer of InAs QDashes grown on S-doped InP(001) substrate in an EIKO gas source molecular-beam epitaxy system and embedded between two $\text{In}_{0.53}\text{Ga}_{0.23}\text{Al}_{0.24}\text{As}$ layers, lattice matched to InP (grown at 500 °C). The dashes were grown in Stransky-Krastanow mode by depositing a 1.3 nm nominal thickness layer of InAs at 470 °C. The entire structure is terminated with a 10 nm-thick layer of InP. The structural data on a QDash morphology show a triangular shape in cross-section of about 20 nm in base width and 3.5 nm in height, whereas the length is estimated to be in between 50 to hundreds of nanometers.²² Since the areal density of QDashes is rather high (above $5 \times 10^{10} \text{ cm}^{-2}$), electron beam lithography and reactive ion etching techniques have been used to pattern the mesa structures with different areas down to $0.2 \mu\text{m}^2$ ($600 \times 300 \text{ nm}^2$) in order to resolve emission from a single QDash from an inhomogeneous ensemble.

In the microphotoluminescence (μPL) experiments, the sample was mounted in the continuous-flow liquid-helium magneto-cryostat and kept at temperature of approximately 5 K. The superconducting magnet is able to generate magnetic field of up to $B = 5 \text{ T}$ and using special sample holders both configurations of the field vector with respect to the optical axis or sample growth axis (z -axis) are accessible: $B \perp z$ and $B \parallel z$. For the purpose of this work, we carried out μPL measurements with magnetic field within the (110) plane (Voigt configuration) with spatial resolution of a single μm using a microscope objective of $\text{NA} = 0.4$. Spectral resolution below $30 \mu\text{eV}$ is provided by a one-meter focal length monochromator. Sub-micrometer etched mesas containing less than fifty QDashes were excited nonresonantly by a cw semiconductor laser diode at 660 nm, and emission intensity of spectral lines was integrated by a liquid nitrogen-cooled InGaAs linear detector. The pre-characterization methodology used here is based on collecting the emission spectra measured as a function of the excitation power density and linear polarization angle. Such data enable us to identify potential candidates for excitons and biexcitons, due to combination of characteristic features such as intensity versus excitation power slope according to simple rate equation model³¹ and symmetric pattern of fine structure as a function of polarization angle.³² Then we perform a single photon cross-correlation experiment that allows us to identify biexciton-exciton cascade, indicating their origin from the same QDash. Later, we cross-correlate the single photon emission events of a given exciton with the surrounding spectral lines with unresolved splitting and approximately linear slope of excitation power dependence to identify the trions unambiguously. Such methodology allowed us to establish the emission pattern that is similar over available spectral range of a given ensemble, establishing the binding energies of biexciton and trion of about $3.5 \pm 0.1 \text{ meV}$ and $4.2 \pm 0.1 \text{ meV}$, respectively, examples of which have been presented elsewhere.^{23,33} The trion is likely to be negatively charged rather than positively charged, as typically extra electron-electron repulsive

Coulomb interaction is much weaker than electron-hole attractive one, which in total enhances the binding energy of the complex, oppositely to positive trion.³⁴ Moreover, the MBE layers deposited on InP substrates show typically n-type background doping in the order of 10^{15} cm^{-3} ,³⁵ supporting the excess of electrons in the vicinity of the QDash layer.

In Figure 1(a), the spectra with emission lines originating from exciton and biexciton confined in a single dash for several magnetic fields are presented. The zero-field energy of the exciton line is 0.79780 meV , which corresponds to $\sim 1554 \text{ nm}$. The absolute value of the fine structure splitting is estimated to be $60 \mu\text{eV}$ from polarization-resolved microphotoluminescence spectra (full polarizer angle rotation) and corresponding to energy difference between the linearly polarized components—two perpendicular orientations with respect to the main axes of a QDash, namely [110] and [1-10]. As the lower energy line is polarized along [1-10], i.e., the dash elongation, which can be easily distinguished by higher intensity for these dashes due to non-zero degree of linear polarization,²¹ it suggests the negative exciton fine structure splitting following the assumption made by Sequin *et al.*¹⁶ for nanostructures elongated in [1-10] direction in the InAs/GaAs material system. When the in-plane magnetic field ($B \perp z$) is applied, the energy separation of the orthogonally polarized components of both X and XX decreases well below $10 \mu\text{eV}$ at 2 Tesla, i.e., within the fitting accuracy by Lorentzian functions. Above the critical field intensity,

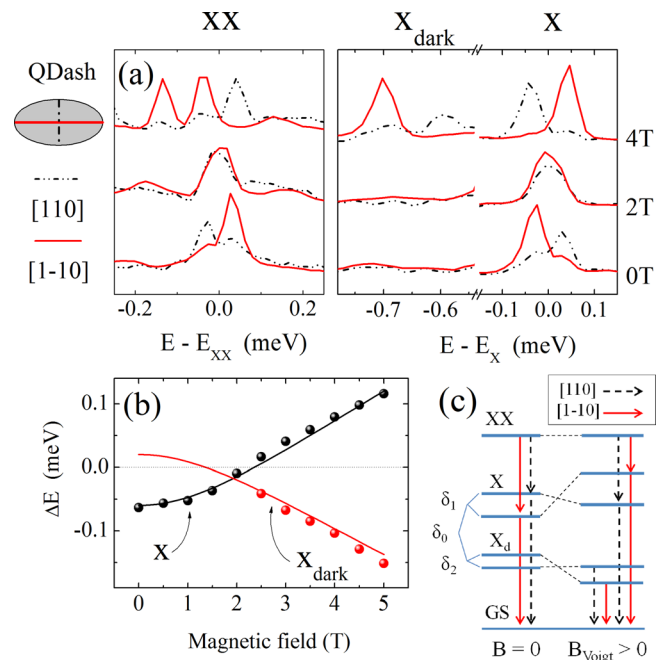


FIG. 1. (a) High-resolution microPL spectra of exciton and biexciton complexes for 0, 2, and 4 T of the in-plane magnetic field. Orthogonal linear polarization are distinguished by red (solid) and black (dash) peaks for [1-10] and [110] axes, respectively. At 2 Tesla, the magnitude of FSS drops down below $10 \mu\text{eV}$, and further Zeeman shift reorders the polarization confirming crossing of exciton states. (b) Zeeman splitting of bright and dark exciton reaching minimum error by using $\delta_1 < 0$ and $\delta_{0,2} > 0$. (c) Biexciton and exciton cascade of linearly polarized transitions and their exchange when in-plane magnetic field is applied, as well as the activation of transitions from dark states due to mixing with bright excitons.

the order of excitonic states is exchanged, indicating the crossing to occur between 2 and 3 T, and evidencing efficient elimination of the exciton spin splitting (Fig. 1(b)). Although the biexciton state is a spin singlet, the replica of crossing dependence has been observed, as the presence of the fine structure is determined by the final exciton state. All the presented figures are shown using relative energy scale with the diamagnetic shift subtracted. In addition, we observe other polarized lines on the lower energy side, shifted by about 0.7 meV with respect to the exciton line, that are attributed to recombination from dark states. The dark exciton states

become optically active in the in-plane magnetic field due to the mixing effect with their bright excitonic counterparts.

The Zeeman splitting of the exciton lines has been determined using the energy difference of the respective excitonic components in the magnetic field

$$\Delta E_{Zeeman} = E_{BX+} - E_{BX-}, \quad (1)$$

and plotted in Fig. 1(b), where the energy of a single bright exciton state has been evaluated according to a standard formula, neglecting quadratic terms related to the diamagnetic shift, as follows:³⁶

$$E_{BX\pm} = E_X(0) + \frac{1}{4} \left[\pm(\delta_1 + \delta_2) + \sqrt{(2\delta_0 \pm \delta_1 \mp \delta_2)^2 + [2(g_{e,x} \mp g_{h,x})\mu_B B]^2} \right]. \quad (2)$$

To proceed with an appropriate fitting procedure and find the exact crossing point in magnetic field dependence, it is necessary to know the in-plane electron and hole g-factors, the isotropic exchange parameter δ_0 and anisotropic term δ_2 related to zero field dark-bright splitting, and dark-dark splitting, respectively, while δ_1 is experimentally determined bright-bright splitting. Both g-factors can be derived directly from the charged exciton Zeeman quadruplet coming from the same dash, and using the formula for its inner and outer components

$$\Delta E_{CX_{in}^{out}} = (g_{e,x} \pm g_{h,x})\mu_B B. \quad (3)$$

We analyzed the charged exciton emission (Fig. 2) and obtained g-factors of $g_{e,x} = |2.06|$ and $g_{h,x} = |0.6|$ which have further been employed in Eq. (2), as both exciton and trion have one electron and one hole magnetically active.³⁷

Subsequently, we have determined the best fit to the experimental data, yielding the exciton zero-field energy of 0.7976 eV and the exchange splittings of $\delta_1 = -60 \mu\text{eV}$, $\delta_2 = 20 \mu\text{eV}$, and $\delta_0 = 420 \mu\text{eV}$. It should be noted that the dark exciton states become visible above 3 T (X_d in Fig. 1(a)). The energy of the dark exciton states is given by

$$E_{DX\pm} = E_X(0) - \frac{1}{4} \left[\mp(\delta_1 + \delta_2) + \sqrt{(2\delta_0 \pm \delta_1 \mp \delta_2)^2 + [2(g_{e,x} \mp g_{h,x})\mu_B B]^2} \right]. \quad (4)$$

Extrapolation of the energy difference between the two split components to zero magnetic field suggests a positive δ_2 in the same nomenclature used for δ_1 sign, as shown in Fig. 1(b). In Figures 1(c) and 2(c), we have illustrated the energy level diagram of the discussed complexes, biexciton-exciton cascade, dark exciton, and charged exciton transitions with and without the influence of external magnetic field. All of these spectroscopic data allowed us to reconstruct the Zeeman splitting curve for excitons subjected to the in-plane magnetic field, and hence, the complete reduction of the bright exciton states splitting at 2.4 T can be expected.

Similar analysis has been performed for several excitons emitting in the range of 1490–1560 nm. The respective fine structure splitting absolute values in the range from 50 to 170 μeV have been detected for these lines. In all the cases, the magnetic field initiates the splitting reduction which confirms unambiguously the negative value of δ_1 . In Figure 3, we show all values of the exciton FSS determined by polarization dependence distributed spectrally according to the position of the exciton emission line (black symbols), and the splitting detected at 5 T for several cases (red symbols).

All final values detected at 5 T convert to positive, proving that the available tuning range is sufficient for cancelling the fine structure splitting of any observed exciton confined in a single quantum dash of the described kind. The largest FSS eliminated by magnetic field is 170 μeV for the exciton line at 0.8312 eV.

We need to note also that FSS does not correlate with excitons energy and degree of linear polarization, as it could be observed in InAs/GaAs quantum dots;¹⁸ thus, we cannot establish any relation between QDash geometry and the observed inversion. According to previous atomistic calculations and the many-body theory employed to InAs/InP nanostructures, their deformation in the plane can lead to the fine structure inversion.^{38,39} However, in the indicated cases, the dots differed significantly from the dashes investigated here in both the sizes and in the lateral aspect ratio. Therefore, this supports our results but can rather serve only as a preliminary indication why the observed negative exciton FSS, which then allowed for its magnetic field tuning down to zero, could be observed for quantum dashes.

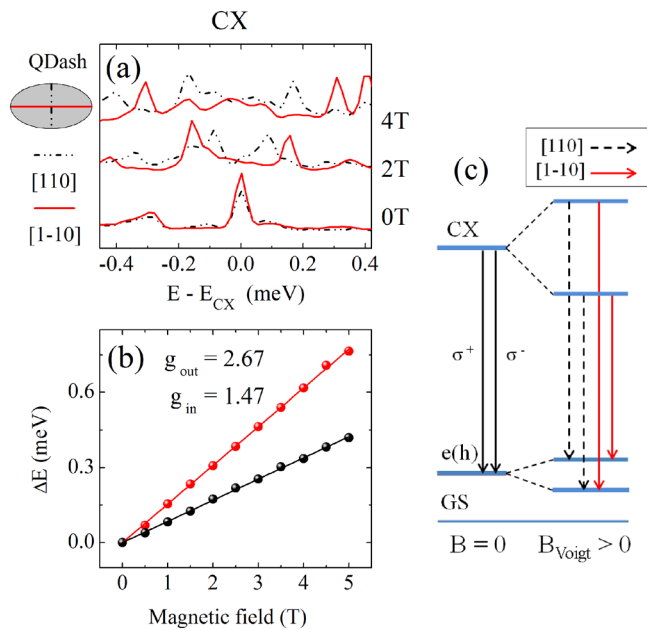


FIG. 2. (a) Polarization resolved spectra of charged exciton showing quadruplet of linearly polarized transitions. (b) Zeeman splitting of outer and inner components corresponding to recalculated electron and hole g -factor of 2.06 and 0.6, respectively. (c) Outline of the charge exciton linearly and circularly polarized transitions with and without in-plane magnetic field, respectively.

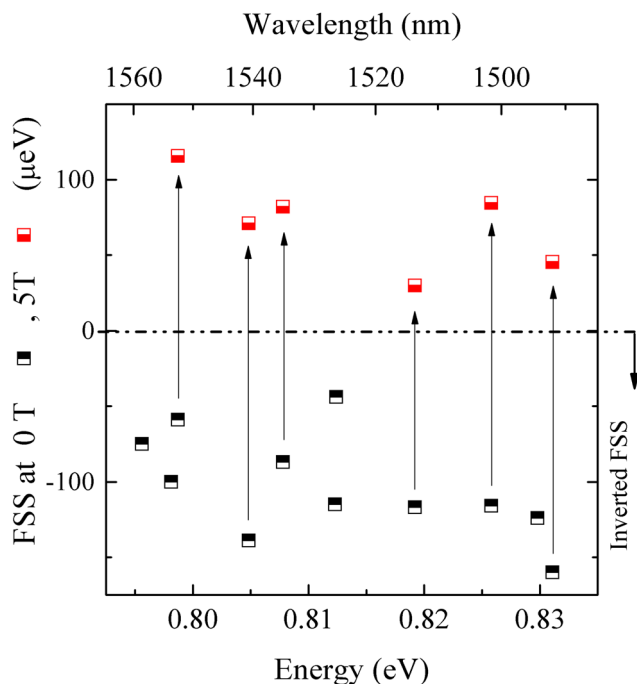


FIG. 3. Zero-field exciton fine structure splitting over spectral range from 1500 nm to 1560 nm, and the final splitting observed at 5 T for several cases. The crossing of states is available for every exciton due to high tuning range of about 150 μeV . Other data support the observation that all excitons are inverted and thus can be tuned to entangled state.

In conclusion, we have investigated the excitonic fine structure in single self-assembled InAs/InGaAlAs/InP quantum dashes under magnetic field up to 5 T in Voigt configuration. Our experimental results show that linear polarization components of the excitonic transitions are reversed in energy,

possibly due to a significant impact of built-in piezoelectric potential on charge carriers captured in relatively large and elongated nanostructures. Applying the in-plane magnetic field, we could achieve a complete elimination of the bright exciton states splitting manifested by the crossing of the magnetic field dependences for the respective lines. This tuning has appeared to be possible for any of the investigated excitons within the entire QDash ensemble emission. These results open up a route for quantum dashes on InP and other anisotropic structures to be applied in sources of entangled photon pairs from the biexciton-exciton cascade or in spin-based quantum memories suitable for fiber-based telecommunication and data transmission technology.

This research was supported by the Polish Ministry of Science and Higher Education/the National Science Center Grant No. 2011/02/A/ST3/00152. The experiments have partially been performed within the laboratory infrastructure financed by the Polish Ministry of Science and Higher Education Grant No. 6167/IA/119/2012. P.M. is a scholar within Sub-measure 8.2.2 Regional Innovation Strategies, Measure 8.2 Transfer of knowledge, Priority VIII Regional human resources for the economy Human Capital Operational Program co-financed by European Social Fund and state budget. S.H. gratefully acknowledges support by the Royal Society and the Wolfson Foundation. We thank E. Harbord for a careful reading of the manuscript.

- ¹H. Briegel, W. Dür, J. Cirac, and P. Zoller, *Phys. Rev. Lett.* **81**, 5932 (1998).
- ²J. Chen, J. Altepetter, M. Medic, K. Lee, B. Gokden, R. Hadfield, S. Nam, and P. Kumar, *Phys. Rev. Lett.* **100**, 133603 (2008).
- ³N. Gisin, G. Ribordy, W. Tittel, and H. Zbinden, *Rev. Mod. Phys.* **74**, 145 (2002).
- ⁴O. Benson, C. Santori, M. Pelton, and Y. Yamamoto, *Phys. Rev. Lett.* **84**, 2513 (2000).
- ⁵A. J. Bennett, M. A. Pooley, R. Stevenson, M. B. Ward, R. B. Patel, A. B. De Giroday, N. Sköld, I. Farrer, C. A. Nicoll, D. A. Ritchie, and A. J. Shields, *Nat. Phys.* **6**, 947 (2010).
- ⁶Y. Shih and C. Alley, *Phys. Rev. Lett.* **61**, 2921 (1988).
- ⁷M. Abbarchi, C. Mastrandrea, T. Kuroda, T. Mano, K. Sakoda, N. Koguchi, S. Sanguinetti, A. Vinattieri, and M. Gurioli, *Phys. Rev. B* **78**, 125321 (2008).
- ⁸K. Kowalik, O. Krebs, A. Lemaître, S. Laurent, P. Senellart, P. Voisin, and J. A. Gaj, *Appl. Phys. Lett.* **86**, 041907 (2005).
- ⁹R. Stevenson, R. Young, P. See, D. Gevaux, K. Cooper, P. Atkinson, I. Farrer, D. A. Ritchie, and A. J. Shields, *Phys. Rev. B* **73**, 033306 (2006).
- ¹⁰R. Singh and G. Bester, *J. Phys. Conf. Ser.* **245**, 012008 (2010).
- ¹¹S. Seidl, M. Kroner, A. Högele, K. Karrai, R. J. Warburton, A. Badolato, and P. M. Petroff, *Appl. Phys. Lett.* **88**, 203113 (2006).
- ¹²W. Langbein, P. Borri, and U. Woggon, *Phys. Rev. B* **69**, 161301 (2004).
- ¹³R. Singh and G. Bester, *Phys. Rev. Lett.* **104**, 196803 (2010).
- ¹⁴M. A. Pooley, A. J. Bennett, R. Stevenson, A. J. Shields, I. Farrer, and D. A. Ritchie, *Phys. Rev. Appl.* **1**, 024002 (2014).
- ¹⁵J. D. Plumhof, V. Krápek, F. Ding, K. D. Jöns, R. Hafenbrak, P. Klenovský, A. Herklotz, K. Dörr, P. Michler, A. Rastelli, and O. G. Schmidt, *Phys. Rev. B* **83**, 121302 (2011).
- ¹⁶R. Seguin, A. Schliwa, S. Rodt, K. Potschke, U. W. Pohl, and D. Bimberg, *Phys. Rev. Lett.* **95**, 257402 (2005).
- ¹⁷R. Stevenson, R. J. Young, P. Atkinson, K. Cooper, D. A. Ritchie, and A. J. Shields, *Nature* **439**, 179 (2006).
- ¹⁸C. H. Lin, W. T. You, H. Y. Chou, S. J. Cheng, S. Di Lin, and W. H. Chang, *Phys. Rev. B* **83**, 075317 (2011).
- ¹⁹C. Tonin, R. Hostein, V. Voliotis, R. Grousson, A. Lemaître, and A. Martinez, *Phys. Rev. B* **85**, 155303 (2012).

- ²⁰E. Harbord, Y. Ota, Y. Igarashi, M. Shirane, N. Kumagai, S. Ohkuchi, S. Iwamoto, S. Yorozu, and Y. Arakawa, *Jpn. J. Appl. Phys.* **52**, 125001 (2013).
- ²¹A. Musiał, P. Kaczmarkiewicz, G. Sęk, P. Podemski, P. MacHnikowski, J. Misiewicz, S. Hein, S. Höfling, and A. Forchel, *Phys. Rev. B* **85**, 035314 (2012).
- ²²A. Sauerwald, T. Kümmell, G. Bacher, A. Somers, R. Schwertberger, J. P. Reithmaier, and A. Forchel, *Appl. Phys. Lett.* **86**, 253112 (2005).
- ²³Ł. Dusanowski, M. Syperek, P. Mrowiński, W. Rudno-Rudziński, J. Misiewicz, A. Somers, S. Höfling, M. Kamp, J. P. Reithmaier, and G. Sęk, *Appl. Phys. Lett.* **105**, 021909 (2014).
- ²⁴M. Bayer, T. Gutbrod, A. Forchel, M. Michel, R. Steffen, and K. H. Wang, *Phys. Rev. B* **58**, 4740 (1998).
- ²⁵V. D. Kulakovskii, G. Bacher, R. Weigand, T. Kümmell, A. Forchel, E. Borovskaya, K. Leonardi, and D. Hommel, *Phys. Rev. Lett.* **82**, 1780 (1999).
- ²⁶B. J. Witek, R. W. Heeres, U. Perinetti, E. P. A. M. Bakkers, L. P. Kouwenhoven, and V. Zwiller, *Phys. Rev. B* **84**, 195305 (2011).
- ²⁷D. Y. Oberli, *Phys. Rev. B* **85**, 155305 (2012).
- ²⁸D. D. Awschalom, D. Loss, and N. Samarth, *Semiconductor Spintronics and Quantum Computation* (Springer-Verlag, Heidelberg, 2002).
- ²⁹D. Press, K. De Greve, P. L. McMahon, T. D. Ladd, B. Friess, C. Schneider, M. Kamp, S. Höfling, A. Forchel, and Y. Yamamoto, *Nat. Photonics* **4**, 367 (2010).
- ³⁰K. De Greve, P. L. McMahon, D. Press, T. D. Ladd, D. Bisping, C. Schneider, M. Kamp, L. Worschech, S. Höfling, A. Forchel, and Y. Yamamoto, *Nat. Phys.* **7**, 872 (2011).
- ³¹G. Sęk, A. Musiał, P. Podemski, and J. Misiewicz, *J. Appl. Phys.* **108**, 033507 (2010).
- ³²Ł. Dusanowski, A. Golnik, M. Syperek, M. Nawrocki, G. Sęk, J. Misiewicz, T. W. Schlereth, C. Schneider, S. Höfling, M. Kamp, and A. Forchel, *Appl. Phys. Lett.* **101**, 103108 (2012).
- ³³Ł. Dusanowski, M. Syperek, W. Rudno-Rudziński, P. Mrowiński, G. Sęk, J. Misiewicz, A. Somers, J. P. Reithmaier, S. Höfling, and A. Forchel, *Appl. Phys. Lett.* **103**, 253113 (2013).
- ³⁴U. W. Pohl, R. Seguin, S. Rodt, A. Schliwa, K. Pötschke, and D. Bimberg, *Phys. E (Amsterdam, Neth.)* **35**, 285 (2006).
- ³⁵P. A. Postigo, M. L. Dotor, P. Huertas, D. Golmayo, and F. Briones, *J. Appl. Phys.* **77**, 402 (1995).
- ³⁶M. Bayer, G. Ortner, O. Stern, A. Kuther, A. Gorbunov, A. Forchel, P. Hawrylak, S. Fafard, K. Hinzer, T. Reinecke, S. Walck, J. Reithmaier, F. Klopff, and F. Schäfer, *Phys. Rev. B* **65**, 195315 (2002).
- ³⁷J. Finley, D. Mowbray, M. Skolnick, A. Ashmore, C. Baker, A. Monte, and M. Hopkinson, *Phys. Rev. B* **66**, 153316 (2002).
- ³⁸L. He, M. Gong, C.-F. Li, G.-C. Guo, and A. Zunger, *Phys. Rev. Lett.* **101**, 157405 (2008).
- ³⁹M. Zieliński, *Phys. Rev. B* **88**, 155319 (2013).